

Research



Cite this article: Kim H *et al.* 2018

Inter-decadal variability of phytoplankton biomass along the coastal West Antarctic Peninsula. *Phil. Trans. R. Soc. A* **376**: 20170174. <http://dx.doi.org/10.1098/rsta.2017.0174>

Accepted: 19 March 2018

One contribution of 14 to a theme issue 'The marine system of the West Antarctic Peninsula: status and strategy for progress in a region of rapid change'.

Subject Areas:

oceanography, biogeochemistry

Keywords:

West Antarctic Peninsula, chlorophyll-*a*, phytoplankton, El Niño–Southern Oscillation, Southern Annular Mode

Author for correspondence:

Hyewon Kim

e-mail: hk8m@virginia.edu

[†]Present address: Department of Environmental Sciences, University of Virginia, Charlottesville, VA 22904, USA.

Electronic supplementary material is available online at <https://doi.org/10.6084/m9.figshare.c.4054925>.

Inter-decadal variability of phytoplankton biomass along the coastal West Antarctic Peninsula

Hyewon Kim^{1,†}, Hugh W. Ducklow¹, Doris Abele², Eduardo M. Ruiz Barlett³, Anita G. J. Buma^{4,5}, Michael P. Meredith⁶, Patrick D. Rozema⁴, Oscar M. Schofield⁷, Hugh J. Venables⁶ and Irene R. Schloss^{3,8,9}

¹Lamont-Doherty Earth Observatory, Columbia University, Palisades, NY 10964, USA

²Alfred Wegener Institute for Polar and Marine Research, Am Handelshafen 12, 27570 Bremerhaven, Germany

³Instituto Antártico Argentino, 25 de Mayo 1143, San Martín Pcia. de Buenos Aires C1064AAF, Argentina


⁴Department of Ocean Ecosystems, Energy and Sustainability Research Institute Groningen, and ⁵Arctic Centre, University of Groningen, Groningen, The Netherlands

⁶British Antarctic Survey, High Cross, Madingley Road, Cambridge, UK

⁷Rutgers University's Center for Ocean Observing Leadership (RU COOL), Department of Marine and Coastal Sciences, School of Environmental and Biological Sciences, Rutgers University, New Brunswick, NJ 80901, USA

⁸Centro Austral de Investigaciones Científicas, Bernardo Houssay 200, Ushuaia, Tierra del Fuego 9410, Argentina

⁹Universidad Nacional de Tierra del Fuego, H. Yrigoyen 879, Ushuaia, Tierra del Fuego 9410, Argentina

 HK, 0000-0002-1280-3340; HWD, 0000-0001-9480-2183; MPM, 0000-0002-7342-7756

The West Antarctic Peninsula (WAP) is a climatically sensitive region where periods of strong warming have caused significant changes in the marine ecosystem and food-web processes. Tight coupling between phytoplankton and higher trophic levels implies that the coastal WAP is a bottom-up controlled system, where changes in phytoplankton dynamics

may largely impact other food-web components. Here, we analysed the inter-decadal time series of year-round chlorophyll-*a* (Chl) collected from three stations along the coastal WAP: Carlini Station at Potter Cove (PC) on King George Island, Palmer Station on Anvers Island and Rothera Station on Adelaide Island. There were trends towards increased phytoplankton biomass at Carlini Station (PC) and Palmer Station, while phytoplankton biomass declined significantly at Rothera Station over the studied period. The impacts of two relevant climate modes to the WAP, the El Niño-Southern Oscillation and the Southern Annular Mode, on winter and spring phytoplankton biomass appear to be different among the three sampling stations, suggesting an important role of local-scale forcing than large-scale forcing on phytoplankton dynamics at each station. The inter-annual variability of seasonal bloom progression derived from considering all three stations together captured ecologically meaningful, seasonally co-occurring bloom patterns which were primarily constrained by water-column stability strength. Our findings highlight a coupled link between phytoplankton and physical and climate dynamics along the coastal WAP, which may improve our understanding of overall WAP food-web responses to climate change and variability.

This article is part of the theme issue 'The marine system of the West Antarctic Peninsula: status and strategy for progress in a region of rapid change'.

1. Introduction

The West Antarctic Peninsula (WAP) is one of the most rapidly warming regions in the Southern Hemisphere, with atmospheric and surface ocean warming especially evident from the 1950s to the late 1990s [1–6]. In accord with atmospheric warming, significant changes in sea ice-, upper ocean- and freshwater dynamics have been reported in the WAP. The timing and duration of the annual sea ice cover have been greatly impacted, showing a significant trend of decreased winter sea ice duration [7]. For the last 50 years, nearly 80% of the glaciers have been in retreat with an accelerating rate of the retreat [8], contributing to increased glacial discharge and freshwater input into the coastal WAP [9,10]. The increased frequency of relatively warm (approx. 2°C) Upper Circumpolar Deep Water delivered onto the WAP continental shelf drives subsurface ocean warming [11]. Superimposed on the aforementioned responses of the WAP system to long-term climate change is strong inter-annual variability of the physical processes, which are driven primarily by two specific modes of climate variability: the Southern Annular Mode (SAM) and the El Niño-Southern Oscillation (ENSO) [12]. The SAM is the dominant mode of extratropical atmospheric variability defined as differences between sea-level pressure anomalies in mid- and high latitudes, which accounts for approximately 35% of the total Southern Hemisphere climate variability [13,14]. Under negative SAM conditions, the WAP region is impacted by cold southerly winds and becomes a favourable environment for sea ice growth and duration (e.g. late spring retreat and early autumn advance) [7]. Similarly, El Niño conditions generate colder periods in the WAP, promoting sea ice growth and duration [7]. Conversely, under La Niña and/or positive SAM conditions sea ice formation is delayed together with shortening of sea ice duration [7].

The changes in upper ocean dynamics affect the ecology and physiology of individual marine organisms as well as whole communities via ecological food-web interactions, given that biological functions and processes are strongly dependent on sea ice dynamics [15]. In particular, phytoplankton responses to climate variability are strongly modulated by sea ice and upper ocean physics. In the coastal WAP, macro- and micronutrient (e.g. iron) concentrations are typically abundant as a consequence of water-column mixing, sedimentary inputs and glacial run-off, thereby not limiting phytoplankton growth [16–21]. In the coastal waters even during the periods peak phytoplankton concentrations, iron usually remains above limiting levels [22]. Phytoplankton growth initiates in the spring after a period of near to total darkness during the Austral winter. The bloom is triggered by increased irradiance within the stabilized water column as a result of solar warming and freshening from spring sea ice melt [2,23–27]. The strength

of water-column stability is predominantly determined by the amount of winter sea ice, which determines the amount of spring sea melt [25]. In this aspect, the inter-annual variability of phytoplankton biomass accumulation is fundamentally shaped by variations in the SAM and ENSO phases. Along the coastal WAP, stronger phytoplankton blooms were consistently reported in conjunction with heavier and more persistent winter sea ice in response to El Niño and/or negative SAM events during the preceding winter [26,28–31]. Besides its inter-annual variability, phytoplankton biomass has undergone a significant long-term change since the 1970s, with opposite trends in the northern and southern WAP regions [32]. The main driver for such trends up to year 2006 is decreasing sea ice cover, which elicits different responses from phytoplankton depending on local environmental conditions. In the northern WAP (near Carlini Station (PC)), increased clouds and more vigorous wind-mixing from reduced sea ice drove a long-term decline in phytoplankton biomass due to reduced water-column stratification [32]. This effect is locally enhanced in shallow coastal areas where mixing causes sediment resuspension, and turbid meltwaters are released by retreating tidewater glaciers as air temperatures rise in the spring as observed at Carlini Station at Potter Cove (PC). By contrast, in the southern WAP (near Rothera Station), increased clouds and more vigorous wind-mixing resulted in a long-term increase in phytoplankton biomass as a shift to open water from nearly permanent ice cover alleviated the shading of phytoplankton cells and exposed them to increased light [32]. With Palmer Station located between the northern and the southern WAP, the findings of Montes-Hugo *et al.* [32] imply a possibility of different phytoplankton responses to physical and climate variability at the three sampling stations along the coastal WAP.

With multi-decadal (i.e. since 1992) datasets from sampling stations along the coastal WAP, our understanding of the long-term phytoplankton variability has been gradually enhanced in recent years. In this study, we present the results from a temporally extensive analysis of phytoplankton biomass datasets collected from three different sampling locations along the coastal WAP: Carlini Station (PC) on King George Island, Palmer Station on Anvers Island and Rothera Station on Adelaide Island. Chlorophyll-*a* (Chl) data have been collected year-round (January–December) for the past 25 years (1992–2016) at Carlini Station (PC) and Palmer Station and for the past 19 years (1998–2016) at Rothera Station. Previous studies on phytoplankton variability at each site addressed significant trends towards increased spring–summer phytoplankton biomass at Palmer Station [33], decreased summer and winter phytoplankton biomass at Rothera Station [31], and some isolated high-biomass events at Carlini Station (PC) and a neighbouring bay on King George Island [28]. Compared to previous separate analyses for each site, our study additionally synthesizes phytoplankton datasets from all three sites together in a large geographical and climate context along the coastal WAP. With both seasonally and annually extended analysis for the three sites, we aim to explore (i) the inter-annual variability of distinct seasonal phytoplankton patterns from each site and (ii) the inter-annual variability of distinct seasonal phytoplankton patterns obtained by considering all three sites together (i.e. incorporating site-specific phytoplankton dynamics and its co-occurrence with the other two sites). In addition, these inter-annual/seasonal covariability patterns of phytoplankton biomass are mechanistically explained in the context of local and regional physical and climate forcings responsible for shaping the observed variability.

2. Material and methods

(a) Site description

The three sampling stations explored in the present study are Carlini Station (PC) on King George Island, Palmer Station on Anvers Island and Rothera Station on Adelaide Island, all located along the coastal WAP (figure 1). Potter Cove is a 7 km² fjordic system of the bigger Maxwell Bay, located in the southwestern end of King George Island (25 de Mayo), South Shetland Archipelago (62°14' S, 58°38' W). The cove is strongly influenced by the retreating Fourcade glacier and a shallow (less than 30 m) sill. This sill traverses the cove close to its mouth, separating the inner

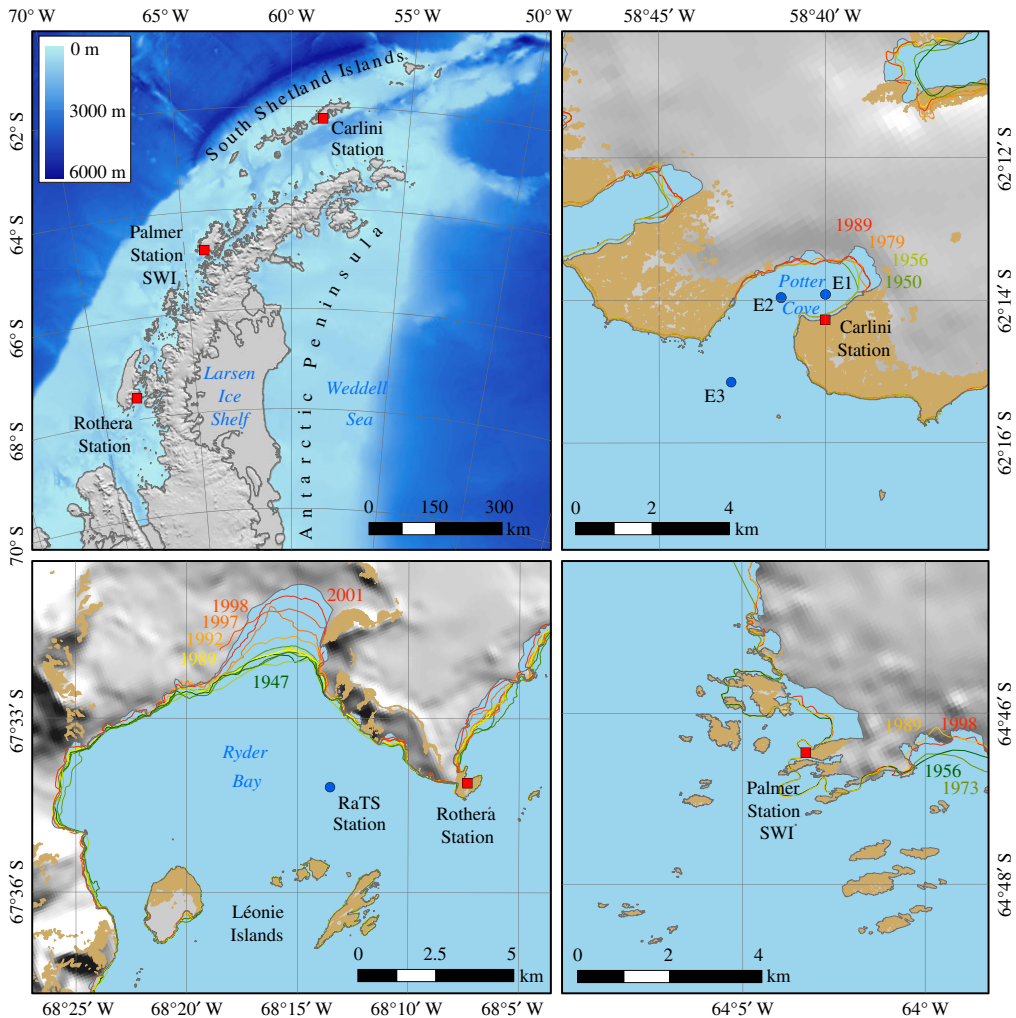


Figure 1. Map of sampling area: the positions of Carlini Station at Potter Cove (PC), Palmer Station seawater intake (SWI) (or Palmer Station) and Rothera Station along the coastal West Antarctic Peninsula (WAP).

(less than 50 m) and outer parts of the cove (approx. 100 m). The central basin of both cove sections (82% of seafloor) is covered by fine sediments and surrounded by shallower rocky areas especially in the outer cove [34]. Potter Cove is influenced by freshwater inputs flowing from two creeks, the Matías and the Potter Creeks, as well as from sediment-loaded subglacial meltwater from the surrounding glacier [35]. More details for Potter Cove are found in Woelfl *et al.* [36] and Schloss *et al.* [26,28,37]. Sampling from three stations, E1 (inner Potter Cove, 62.23° S, 58.67° W), E2 (outer Potter Cove, 62.23° S, 58.69° W) and E3 (Maxwell Bay, 62.25° S, 58.71° W), was carried out biweekly from September to April and monthly during the rest of the year, whenever the meteorological conditions permitted. Palmer Station (64.77° S, 64.05° W) is located on Anvers Island in the coastal WAP. Year-round Chl data have been collected with a submersible pump at the Palmer Station seawater intake (approx. 6 m), located at the end of a short pier in Arthur Harbor [38]. The main Rothera Time Series (RaTS) sampling station (67.34° S, 68.15° W) is located in Ryder Bay, situated approximately 4 km from shore at a water depth of approximately 520 m. A sill at around 300 m depth separates Ryder Bay from the northern part of Marguerite Bay. When samples were not collected due to weather and logistical reasons, data from two adjacent sampling stations, secondary Rothera Station (67.35° S, 68.93° W, approx. 400 m depth) and Biscoe Wharf (67.34° S,

68.80° W, less than 100 m depth), were used instead: further details for sampling protocols and Chl determination are available in electronic supplementary material, Text S1 and S2.

(b) Data treatment

The Chl datasets analysed for all three sampling stations are year-round volumetric Chl concentrations ($\mu\text{g l}^{-1}$) from 5 m depth at Carlini Station (PC) and 6 m depths at Palmer Station and Rothera Station. The data cover the 25 year period (1992–2016) at Carlini Station (PC) and Palmer Station, and the 19 year period (1998–2016) at Rothera Station. For all three stations, duplicate measurements at the same depth were averaged, and extreme outlier values (greater than $30 \mu\text{g l}^{-1}$; 0.7% of total sample size) were removed to avoid biases in the eigenstructure (see §2c Empirical orthogonal function decomposition). Extracted Chl data were used for Carlini Station (PC) and Palmer Station given their availability at similar sampling depths. Given that the bottle data were only measured from 15 m at Rothera Station, we chose to use fluorescence data at 6 m for Rothera Station to ensure consistency of the sampling depths analysed across the three stations. Using fluorescence datasets is not expected to introduce artefacts in the comparisons among the three stations, given the very strong correlation between Chl values from the in-line fluorometer on the CTD and the bottle-extracted Chl values from 15 m, from which routine calibration has been performed at Rothera Station [24,29].

For Carlini Station (PC), raw daily volumetric Chl concentrations were averaged from stations E1–E3 to ensure maximum sample size, given that the patterns from our analysis (e.g. climatology and EOF patterns) did not show considerable differences compared to analyses for only one station, E1 or E2. Schloss *et al.* [26] analysed phytoplankton values above (0–10 m averages) and below the pycnocline (20–30 m averages) in E1 and E2 separately. However, we used an average of Chl values from E1 and E3 to represent spatially more extended features of Potter Cove, from the 5 m depth only, based on no discernable differences in the EOF patterns. The data gaps from Palmer Station were filled with the data from the inshore Palmer Station B based on the correlation between Chl values from these two sites ($r^2 = 0.49$, $p < 0.001$ for raw volumetric Chl data and $r^2 = 0.87$, $p < 0.001$ for \log_{10} -transformed raw volumetric Chl data). The volumetric Chl concentrations for all studied years are characterized by typical lognormal distributions at all three stations ($n = 406$, mean = 0.87, $\sigma = 1.51$ at Carlini Station (PC); $n = 1448$, mean = 2.33, $\sigma = 4.35$ at Palmer Station and $n = 812$, mean = 2.97, $\sigma = 5.31$ at Rothera Station). Non-Gaussian distributed, raw volumetric Chl data were used for calculating monthly standardized anomalies, whereas they were \log_{10} -transformed to ensure that the distributions were as nearly Gaussian distribution as possible for conducting empirical orthogonal function (EOF) analysis (see below and electronic supplementary material, figures S1 and S2).

(c) Empirical orthogonal function decomposition

We employed EOF analysis as a main analytical method. EOF analysis is widely used as a means of quantifying the inter-annual variability about the climatological means of a variable of interest and its spatial variability structure (i.e. spatio-temporal variability) [11]. In our study, EOF analysis was performed in two different ways of setting up the matrix to be eigen-decomposed: (i) months of each year to represent seasons (i.e. January–December) by individual years for each site separately and (ii) months of all three sampling sites (i.e. January–December, ... January–December, ... January–December) by individual years for all three sampling sites together to explore (i) each individual site's seasonal–inter-annual covariability and (ii) seasonal–inter-annual covariability of all three stations together. These two approaches to the EOF analysis are referred to as the first case of the EOF analysis and the second case of the EOF analysis. The first case of the EOF analysis represents seasonal–inter-annual covariability or the inter-annual variability of seasonal progression of phytoplankton biomass at each sampling station. The second case of the EOF analysis reveals not only each sampling station's specific dynamics but also its interactions with the other two stations in a statistical manner. Detailed explanation for matrix notation and equations are available in electronic supplementary material, Text S3.

(d) Statistical analyses

Linear trends in the Principal Component (PC) time series and actual Chl data were examined parametrically at a statistical significance level of $p < 0.05$, testing against the null hypothesis that the slope coefficient (β_1) of the linear regression equation ($Y = \beta_0 + \beta_1 T + \epsilon$) is zero. To examine trends in the actual Chl data, we calculated monthly anomalies (standardized) of Chl to reduce the confounding effects of outlier values and seasonal cycle. Standardized anomalies were calculated as $x - \bar{x}/\bar{s}$, where \bar{x} is the climatological mean and \bar{s} is the climatological standard deviation. Chl composites (averages) during different climate regimes were compared using a one-tailed Student's *t*-test for unpaired samples to address unequal sample size for each distinct climate regime. Owing to small sample sizes ($n=9$ and 15 for El Niño/ $-$ SAM and La Niña/ $+$ SAM), a relaxed criterion was used as the level of statistical significance at $p < 0.10$. The bootstrapped technique was employed to cross-correlations to fix autocorrelation-induced inflation in the sample size (full details in [21]).

(e) Physical and climate variability

Climate variability datasets explored in the present study included the Southern Oscillation Index (SOI), the Multivariate ENSO Index (MEI) and SAM indices. The monthly SOI and MEI indices were downloaded from the National Oceanic and Atmospheric Administration Earth System Research Laboratory website (<http://www.esrl.noaa.gov/psd>). The monthly SAM index was obtained from the British Antarctic Survey (BAS, <http://www.nerc-bas.ac.uk/icd/gjma/sam.html>). For water-column stability parameters at Carlini Station (PC), the Brunt-Väisälä frequency (N^2) between 1 and 25 m depth was calculated. For this analysis, we only considered observations when at least seven samples were collected in each CTD profile (calculation method for N^2 detailed in Schloss *et al.* [26]), while MLD was used for Rothera Station (calculation method detailed in Clarke *et al.* [24]).

3. Results

(a) Climatology, monthly anomalies and trends

(i) Carlini Station

At Carlini Station (PC) phytoplankton biomass was typically low with values ranging from 0.01 to $21.98 \mu\text{g l}^{-1}$ and a 25 year mean value of $0.87 \pm 1.51 \mu\text{g l}^{-1}$ (figure 2*a*). The overall mean value was 4% of the maximum. The climatology showed that the primary peak in Chl occurred during March at $2.29 \pm 3.79 \mu\text{g l}^{-1}$ (figure 3*a*); however, this result might be due to two unusually high values in 2012 ($16.24 \mu\text{g l}^{-1}$ on average, approx. sevenfold larger than the March climatology). After removing these high values, the maxima climatological Chl value was observed in December ($1.49 \mu\text{g l}^{-1}$, data not shown). Monthly anomalies were characterized by three notable patterns (figure 4*a*), showing (i) the magnitude of positive anomalies was generally larger than that of negative anomalies over the studied years, (ii) positive anomalies increased in magnitude and occurred more frequently since 2009 and (iii) the frequency of positive anomalies increased significantly over the 25 year period ($p = 0.005$).

(ii) Palmer Station

Compared with Carlini Station (PC), phytoplankton biomass was relatively higher at Palmer Station, ranging from 0.01 to $29.86 \mu\text{g l}^{-1}$ with a 25-year mean value of $2.33 \pm 4.35 \mu\text{g l}^{-1}$ (figure 2*b*). The 25-year mean corresponded to 7.8% of this maximum value recorded. The climatology revealed one Chl peak in January ($4.90 \pm 4.32 \mu\text{g l}^{-1}$; figure 3*b*). Similar to Carlini Station (PC), the magnitude of positive anomalies was larger than that of negative anomalies

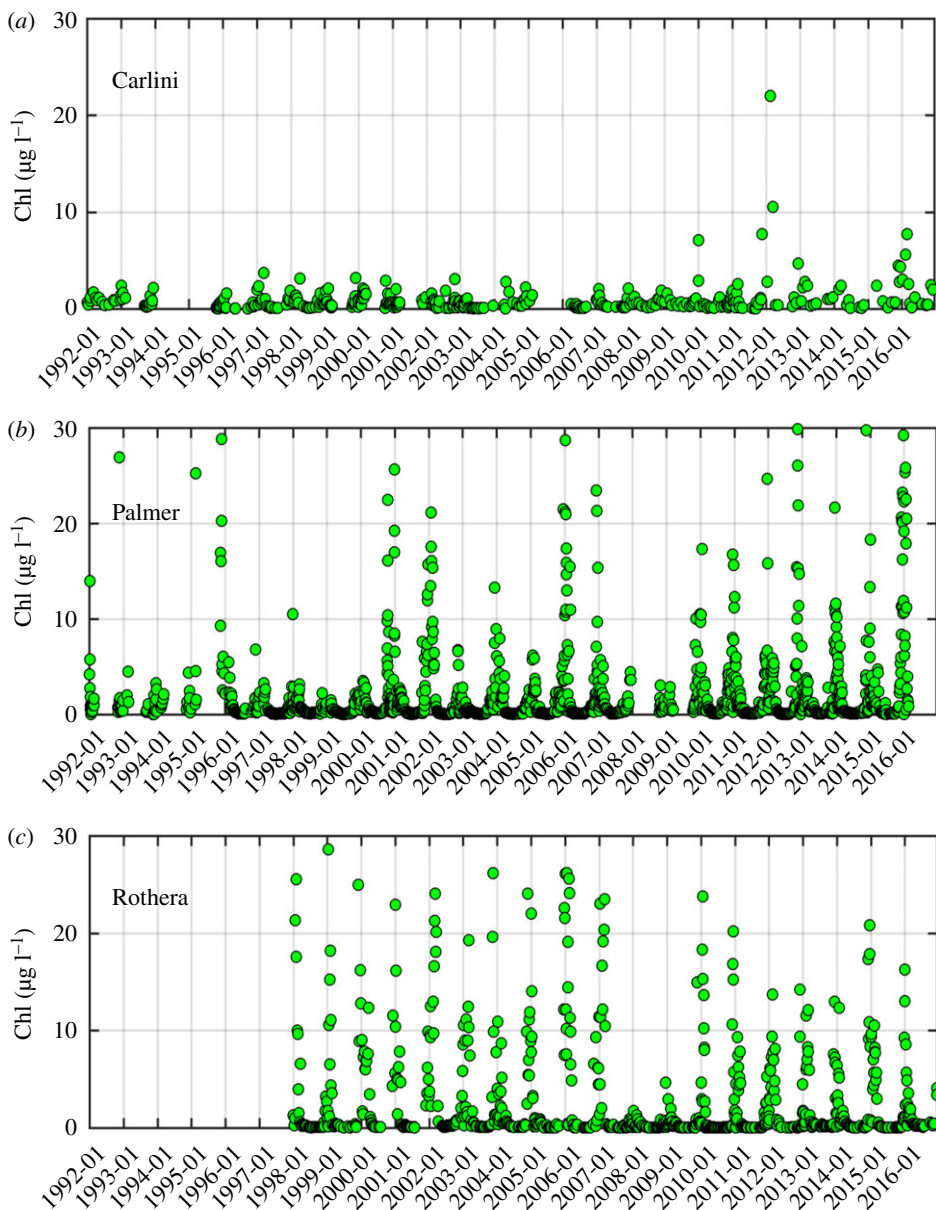


Figure 2. Daily volumetric chlorophyll-*a* (Chl) time series at Carlini Station (PC), Palmer Station and Rothera Station for the studied period. Note that no data are available from 1992 to 1997 at Rothera Station.

over the studied period and more frequent positive anomalies were found since 2010 (figure 4*b*). Accordingly, there was an increasing trend in monthly Chl anomalies ($p = 0.003$).

(iii) Rothera Station

Phytoplankton biomass at Rothera Station was relatively higher than at Carlini Station (PC) but similar to Palmer Station with values ranging from 3.10×10^{-3} to $28.59 \mu\text{g l}^{-1}$ and a 19-year mean value of $2.97 \pm 5.31 \mu\text{g l}^{-1}$ (figure 2*c*). The 19-year mean Chl value corresponded to 10.4% of the maximum. Climatology showed Chl maxima in February ($6.55 \pm 4.61 \mu\text{g l}^{-1}$; figure 3*c*). Compared to Carlini Station (PC) and Palmer Station, there were prolonged high Chl values in spring and summer (December–March), well above the background (winter) concentration. Notably, monthly anomalies at Rothera Station were characterized by a transition from prolonged

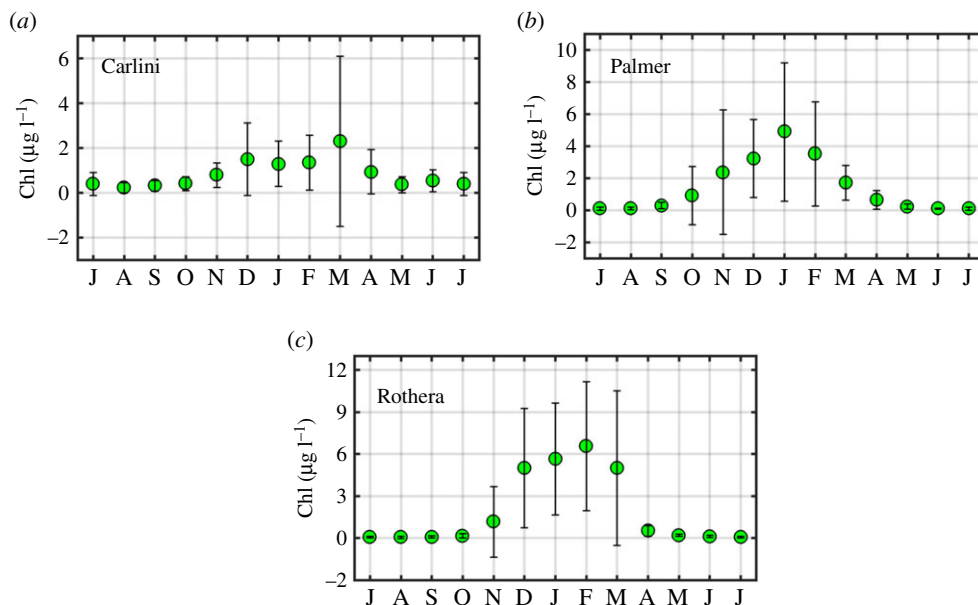


Figure 3. The climatology of Chl at Carlini Station (PC), Palmer Station and Rothera Station for the studied period. Error bars indicate standard deviations. Monthly means for the past 25-year period (1992–2016) were calculated for Carlini Station (PC) and Palmer Station, while monthly means for the past 19-year period (1998–2016) were calculated for Rothera Station. The value in July is presented twice to make monthly Chl values be presented consecutively. (Online version in colour.)

positive (1998–2004) to negative anomalies (2007–2012), followed by a subsequent period of positive and negative anomalies since then (figure 4c). Owing to this period of prolonged negative anomalies, there was a significant decreasing trend in the monthly anomalies at Rothera Station ($p = 0.020$).

(b) The first case of the empirical orthogonal function analysis: seasonal/inter-annual covariability at individual stations

This section focuses on the results from the first case of the EOF analysis (§2c Empirical orthogonal function decomposition, electronic supplementary material, Text S3), describing the patterns of EOF and PC time series at each sampling station. EOF represents distinct variability patterns in the seasonal progression of phytoplankton biomass accumulation, where the first and second EOFs capture the first two dominant, uncorrelated and independent seasonal variability patterns in the Chl datasets. It should be noted that EOF indicates how much phytoplankton biomass in a given month is larger or lower than the climatology of that month. Thus, it is the covariability in deviations from average phytoplankton biomass that is examined, not an actual average biomass pattern at each site. The PC time series represent how these seasonal variability patterns vary inter-annually, representing the inter-annual variability of seasonal phytoplankton dynamics. Yearly Chl anomalies were reconstructed using the first few leading modes (5, 6 and 5 modes for Carlini Station (PC), Palmer Station and Rothera Station, respectively), representing the combined effects of varying phytoplankton bloom phenology on each studied year (electronic supplementary material, figures S3–S5).

(i) Carlini Station

The leading EOF mode (mode 1) captured 38% of the total Chl variability. Mode 1 captured year-round extended and prolonged, positive Chl anomalies from January to December, with a strong phytoplankton biomass peak in February (EOF1; figure 5a). The years with year-round

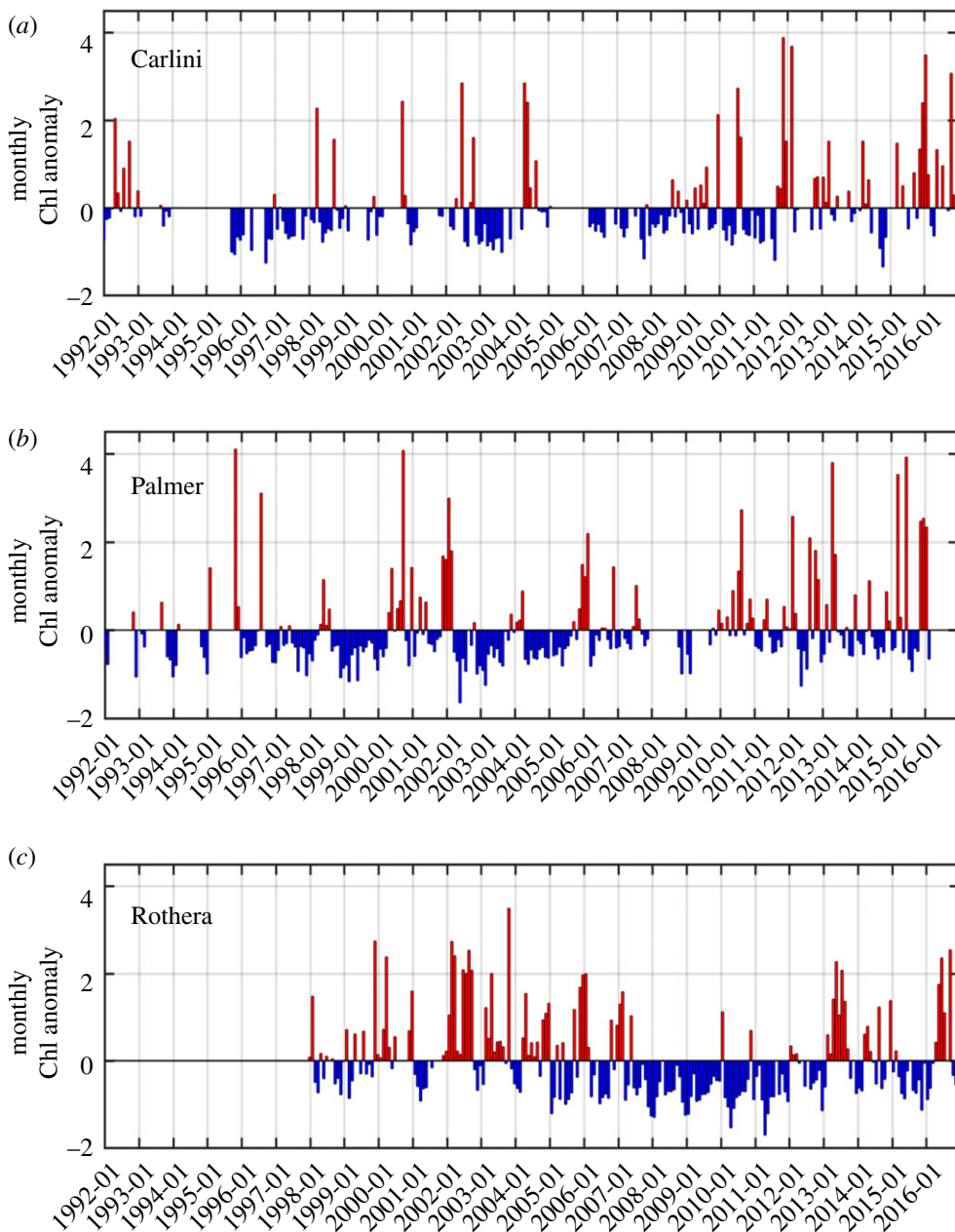


Figure 4. Monthly Chl anomalies at Carlini Station (PC), Palmer Station and Rothera Station for the studied period. Monthly anomalies were calculated as standardized anomalies. Note that no data are available from 1992 to 1997 at Rothera Station.

positive Chl anomalies were represented by the PC1 time series, indicating overall high Chl years throughout all seasons, the year 2003 as the lowest and the year 2016 as the highest Chl year (PC1; figure 5a). No trend was detected from the PC1 time series ($p > 0.05$). The second EOF mode (mode 2) captured 22% of the total Chl variability. Mode 2 described a relatively particular seasonal variability pattern, characterized by an abrupt transition of negative to positive anomalies from August–September to October–December with relatively weak signal in the other months (EOF2; figure 5a). Presenting a typical spring bloom, this pattern was most strongly expressed in 2011 and weakest in 2010 and 2014 (PC2; figure 5a). No trend was detected for the PC2 time series ($p > 0.05$).

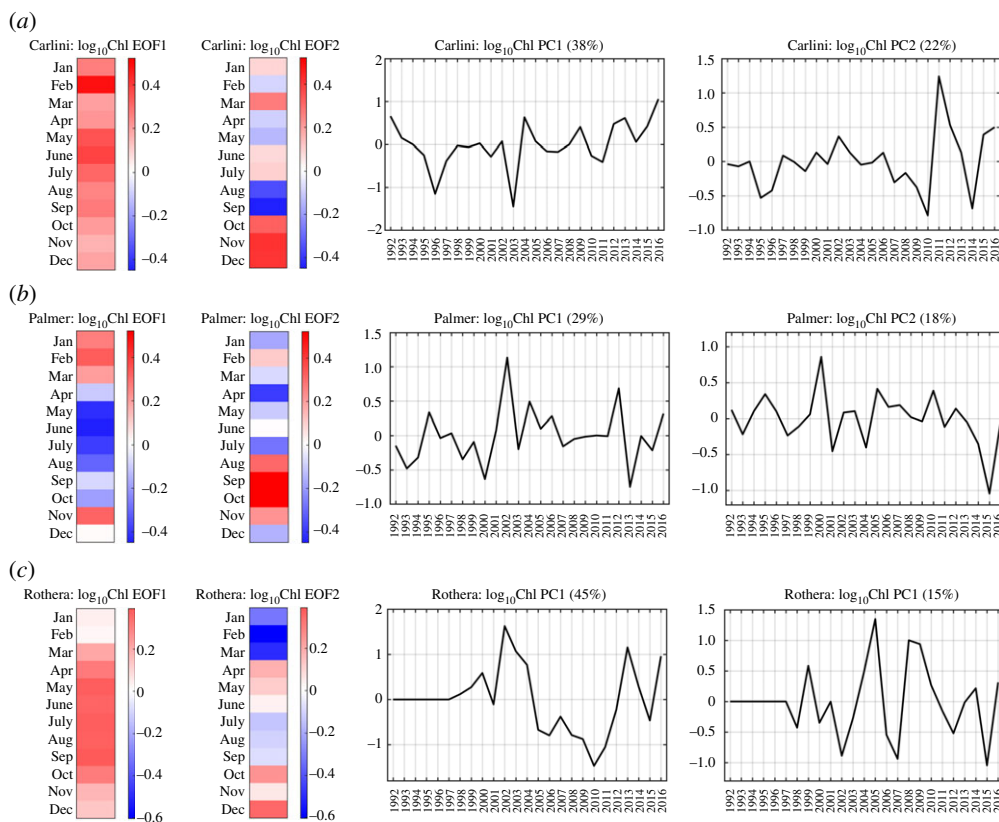


Figure 5. Empirical Orthogonal Function (EOF) and Principal Component (PC) time series of the Chl datasets at individual stations. The set of EOF and PC patterns from the first case of the EOF analysis is presented for (a) Carlini Station (PC), (b) Palmer Station and (c) Rothera Station. The red colours represent positive $\log_{10}\text{Chl}$ anomalies and the blue colours represent negative $\log_{10}\text{Chl}$ anomalies in the EOF plots. The percentage explained by each mode is represented in the corresponding PC time series. Note that no data are available from 1992 to 1997 at Rothera Station.

(ii) Palmer Station

The leading EOF mode (mode 1) captured 29% of the total Chl variability. Mode 1 captured summer phytoplankton blooms (January—March) followed by very low Chl during the Austral winter months (EOF1; figure 5b). No significant trend was found for this pattern (figure 5b, PC1, $p > 0.05$). The second EOF mode (mode 2) captured 18% of the total Chl variability. Mode 2 captured high Chl in the early spring (early spring blooms), contrasting the phenology of the phytoplankton bloom captured by mode 1 (EOF2; figure 5b). The inter-annual variability of the seasonal Chl variability pattern captured by mode 2 appears in the PC2 time series (PC2; figure 5b). No significant trend was found from the PC2 time series ($p > 0.05$). More details of the phytoplankton variability at Palmer Station are found in Kim *et al.* [21].

(iii) Rothera Station

The leading EOF mode (mode 1) captured 45% of the total Chl variability. Mode 1 captured an overall elevated phytoplankton biomass pattern as a year-round positive Chl anomaly (i.e. higher than the 19 year climatology) (EOF1; figure 5c). The year-to-year variability of this seasonal variability pattern was represented in the PC1 time series (PC1; figure 5c). The magnitude of PC1 values consistently decreased from 2002 to 2010. This specific period with the decreasing PC1 partly overlapped with that of the prolonged negative anomalies discussed in Results 3a. Because

mode 1 captured nearly half of the total Chl variability, its effect was strongly reflected in the overall monthly anomaly patterns. There was no long-term trend in the PC1 time series ($p > 0.05$). The second EOF mode (mode 2) captured 15% of the total Chl variability. Mode 2 captured a strong negative Chl anomaly in January–March preceding the second half of the Austral growing season and a positive Chl anomaly in October–December (EOF2; figure 5c). Compared to PC1, PC2 fluctuated markedly, reflecting the abruptly changing inter-annual variability of the seasonal pattern captured by EOF2 (PC2; figure 5c). Similar to Carlini Station (PC) and Palmer Station, there was no long-term trend in the PC2 time series ($p > 0.05$).

(c) The second case of the empirical orthogonal function analysis: seasonal/inter-annual-spatial covariability for all three stations together

This section presents the results from the second EOF analysis, explaining the patterns of the EOF/PC by analysing the Chl data at the three stations together. Thus, EOF captures the seasonal variability patterns in the progression of phytoplankton biomass accumulation, which are statistically derived from concurrent responses of all three stations (i.e. seasonal–inter-annual covariability interacting with spatial variability). Yearly Chl anomalies were reconstructed for each station using the first 10 EOF modes (electronic supplementary material, figures S6–S8).

The leading EOF mode (mode 1) captured 22% of the total Chl variability. Mode 1 captured seasonal–spatial phytoplankton biomass patterns characterized by negative Chl anomalies in January–July and in October–November at Carlini Station (PC), positive Chl anomalies in June–December at Palmer Station (especially high Chl in June–September) and nearly consistent year-round negative Chl anomalies at Rothera Station (EOF1; figure 6a). The year which resembled the EOF1 seasonal pattern most was represented as the highest PC1 (year 2010), while the year 2002 was the lowest PC1 year (PC1; figure 6a). Notably, these two contrasting PC1 years were associated with different climate variability phases. The highest PC1 year was characterized by the strong winter La Niña year (SOI in July 2010 = 1.95 and MEI in August 2010 = –1.67), while the lowest PC1 year was characterized by the strong winter El Niño and negative SAM conditions (SOI in August 2002 = –1.62, MEI in August 2002 = 1.03, and SAM in July 2002 = –0.67). There was no significant trend in the PC1 time series ($p > 0.05$).

The second EOF mode (mode 2) captured 16% of the total Chl variability. In contrast to mode 1, mode 2 captured the low-frequency-dynamics-like feature of the phytoplankton biomass accumulations along the three stations. Mode 2 captured seasonal–spatial phytoplankton biomass patterns characterized by year-round negative Chl anomalies at Carlini Station (PC), prolonged negative Chl anomalies in January–September with an abrupt transition to positive Chl anomalies in the spring (October–December) at Palmer Station and prolonged year-round positive Chl anomalies at Rothera Station (EOF2; figure 6b). No distinct relationship of the PC2 time series to climate variability was observed. However, the PC2 time series showed a weak but significant decreasing trend over the studied years ($p = 0.04$; PC2; figure 6b).

4. Discussion

(a) Climatology, monthly anomalies and trends

Despite geographical proximity (approx. 745 km between Carlini Station (PC) and Rothera Station, which places all three Antarctic stations under similar climatic forcing of atmospheric teleconnection), the three stations were differentiated by distinct features in the seasonal progression of phytoplankton biomass accumulation. The magnitude of the maximum spring/summer phytoplankton biomass at Carlini Station (PC) was notably lower than at Palmer Station and Rothera Station, with approximately threefold lower mean and approximately 2.5-fold lower climatological peak values. Located in light-limited Antarctic waters, phytoplankton dynamics at all three sites are primarily driven by increased irradiance in stabilized water

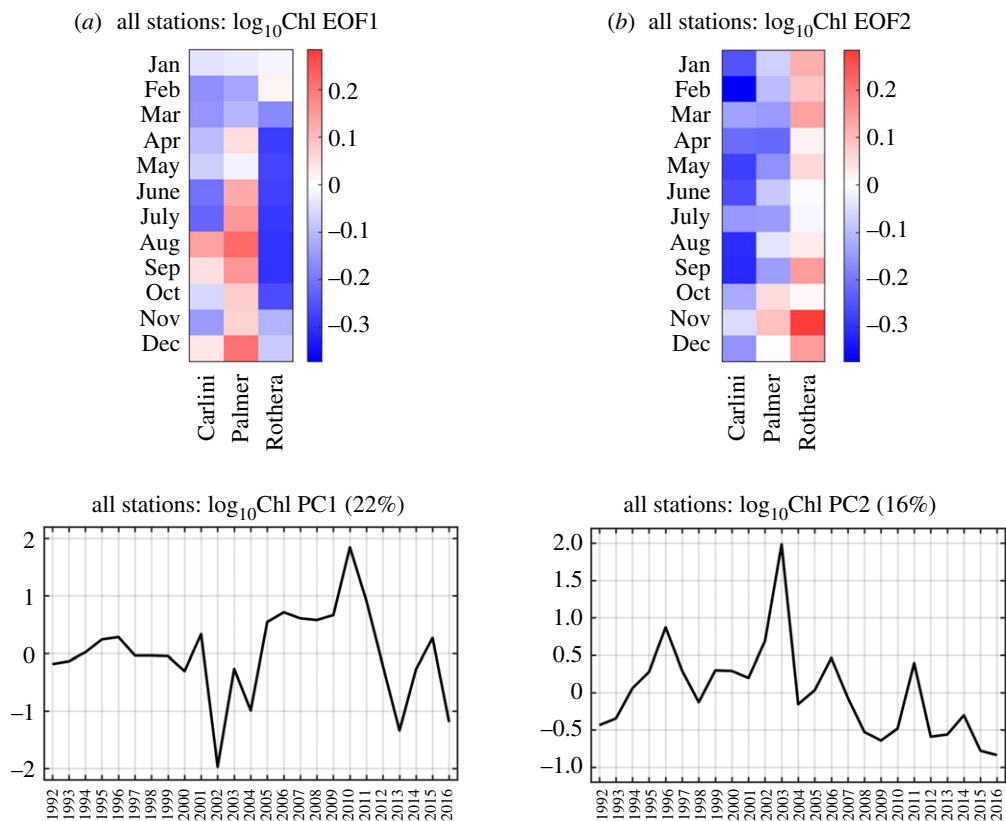


Figure 6. EOF and PC time series of the Chl datasets for all three stations. The set of EOF and PC patterns from the second case of the EOF analysis is presented for the first mode (mode 1, *a*) and the second mode (mode 2, *b*). The red colours represent positive \log_{10} Chl anomalies and the blue colours represent negative \log_{10} Chl anomalies in the EOF plots. The percentage explained by each mode is represented in the corresponding PC time series.

columns, as determined by the amount of spring sea ice melt, glacial meltwater input during summer and the degree of wind-driven turbulent mixing. Along with sufficient macronutrient supply, iron inputs from a variety of sources (e.g. coastal glaciers, bottom sediments and deep water) make iron limitation rare or incidental during the growing seasons (e.g. at the end of summers) at Palmer Station and Rothera Station [10,21,24,28,39,40]. Given similar physical and environmental settings for phytoplankton dynamics at all three stations, significantly lower phytoplankton biomass at Carlini Station (PC) (often less than 1 mg m^{-3} during growing seasons and the occasional maximum less than 5 mg m^{-3}) requires an alternative explanation [26]. Previous studies showed that, in most areas of inner Potter Cove, high loads of suspended particulate organic matter from coastal glacial run-off, melting and sediment resuspension significantly reduce irradiance levels in the water column [26,37,41–43]. Large quantities of lithogenic particulate coastal and subglacial run-off result in an up to 5 m thick turbid surface layer that builds up during the melt season and restricts phytoplankton growth through attenuation of the underwater light climate. The effect of the sediment plume on phytoplankton light-harvesting pigments is significant and rapidly reduces photoprotective capacity in natural phytoplankton once it reaches the turbid water areas of the cove [44]. Schloss *et al.* [42] demonstrated that coastal run-off restricts phytoplankton growth, rather than acting as a positive stimulus for phytoplankton growth by enhanced water-column stability. Lower levels of suspended particulate matter at Palmer Station and Rothera Station might explain the relatively larger magnitudes of phytoplankton biomass compared to Potter Cove.

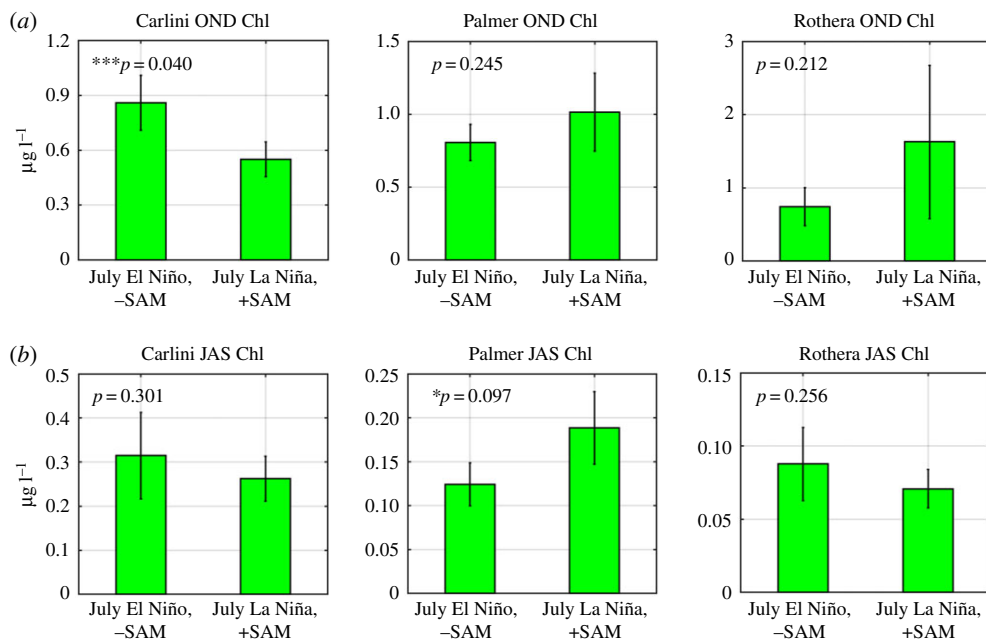


Figure 7. EOF-reconstructed Chl composites during different climate variability regimes. Chl values are reconstructed using the first 5, 6 and 5 dominant modes for Carlini Station (PC), Palmer Station and Rothera Station, respectively. (a) Spring (October–November–December or OND) Chl composites and (b) winter (July–August–September or JAS) Chl composites when preceded by El Niño/–SAM and La Niña/+SAM conditions in July. Owing to small sample sizes ($n = 9$ and 15 for El Niño/–SAM and La Niña/+SAM) in the analyses, a relaxed criterion was used for the level of significance at $p < 0.10$. (Online version in colour.)

Also notable is the opposite sign of the long-term Chl trends at the three stations. Monthly anomaly patterns appeared to be similar between Carlini Station (PC) and Palmer Station, with generally larger amplitudes of positive anomalies than negative anomalies. In addition, at Carlini Station (PC) and Palmer Station, there was an increased frequency of positive anomalies in the recent years (since 2010; see [28,33]), which seems to drive the increasing Chl trends at both sites. Saba *et al.* [30] demonstrated that, in the coastal WAP, positive Chl anomalies during the Austral summer were driven by negative SAM conditions in the preceding winter and positive SAM conditions in the following spring as both climate conditions contribute to increased water-column stability via ice melt and reduced wind stress, respectively. The El Niño phase in the previous winter is known to act similarly as an environmental setting favourable for large phytoplankton blooms as a result of increased winter sea ice growth, spring ice melt and resulting stratification of the upper water column [7,29–31]. In particular, increasing trends of the Chl anomalies at Carlini Station (PC) and Palmer Station were largely influenced by large amplitudes of positive Chl anomalies since 2009–2010. The negative winter SAM condition (SAM in July 2011 = -1.52) might contribute to positive Chl anomalies in the spring at Carlini Station (PC). In contrast, positive Chl anomalies in the spring–summer months (2015 through 2016) at Carlini Station (PC) and Palmer Station might be attributed to very strong El Niño events persisting from the winter (SOI in August 2015 = -1.41 and MEI in August 2015 = 2.37). At Carlini Station (PC) these observations are further supported by significantly increased Chl in the spring as a result of El Niño and negative SAM phases, supporting high winter sea ice growth and spring ice melt (figure 7a). More importantly, at Carlini Station (PC) there is a significant impact of local forcing (i.e. glacial melting), in conjunction with large-scale climate forcing, on controlling phytoplankton biomass. In +SAM/La Niña years due to relatively high air temperatures, increased sedimentary run-off could limit phytoplankton growth and accumulations [45]. Consistent with previous findings [21,30] spring phytoplankton accumulations at Palmer Station were weakly positively

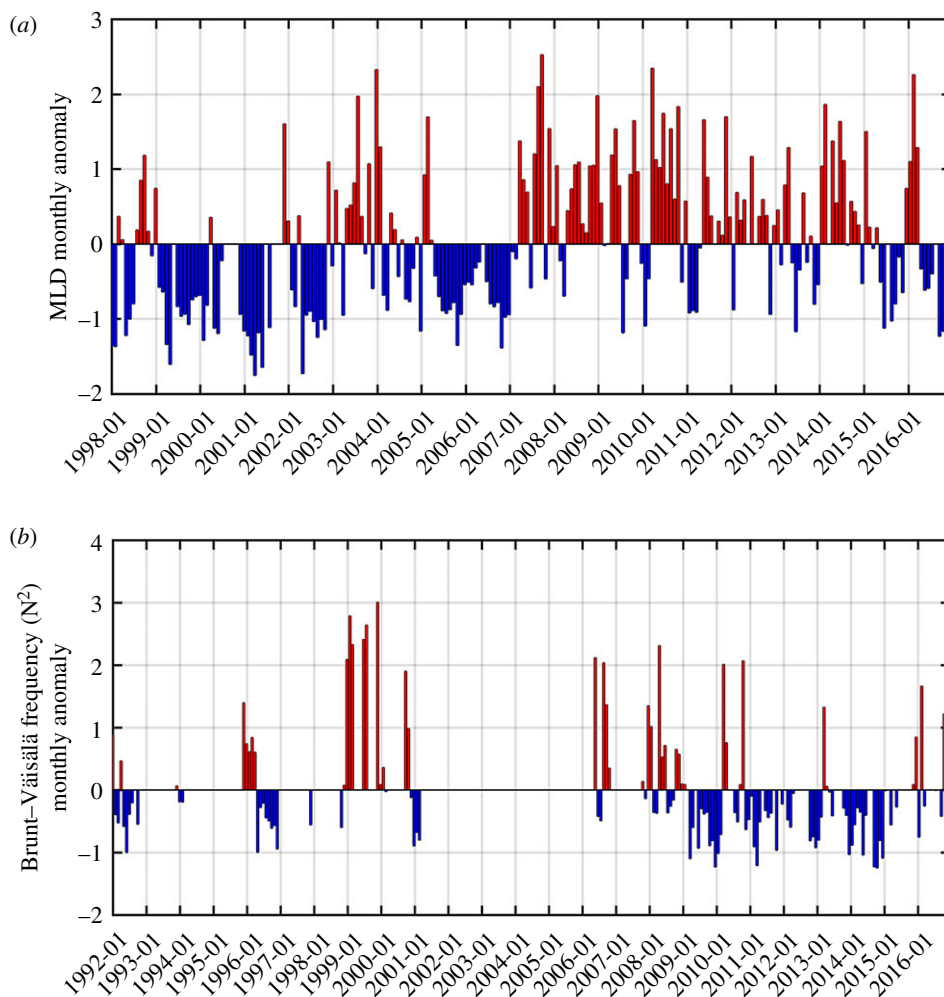


Figure 8. (Continued.)

influenced by negative SAM conditions in the preceding winter ($r = -0.23$, $p = 0.058$ for SAM JJA versus \log_{10} Chl OND). Winter months in the year 2015 were characterized by strong positive SAM conditions (SAM in July 2015 = 2.00 and SAM in August 2015 = 1.86), so it is likely that large phytoplankton accumulations at Palmer Station in the spring of that year was shaped by strong El Niño conditions. However, there was no significant response in the spring phytoplankton biomass at Rothera Station as a function of different ENSO and SAM conditions (figure 7a). Notably, Rothera Station was characterized by an opposite pattern, with an abrupt transition from prolonged positive (1998–2004) to negative anomalies (2007–2012) and therefore a significantly decreasing Chl trend. These low Chl years (2007–2012) are consistent with observations by Rozema *et al.* [31], where they attributed low phytoplankton biomass to reduced winter sea ice and decreased summer stratification strength. Indeed, the period of the low Chl years (2007–2012) corresponded to the prolonged period of deeper MLD (positive MLD anomalies in figure 8a). Venables *et al.* [29] demonstrated that decreased winter ice cover was linked to a deepening of the winter mixed layer and persistently reduced stratification during the following spring–summer. During periods of low winter ice cover, the water column is more deeply mixed and thereby requires more buoyancy to be stabilized. Consistent with previous observations [29,31], there was an increasing trend of monthly MLD anomalies at Rothera Station ($p < 0.001$; figure 8a), which

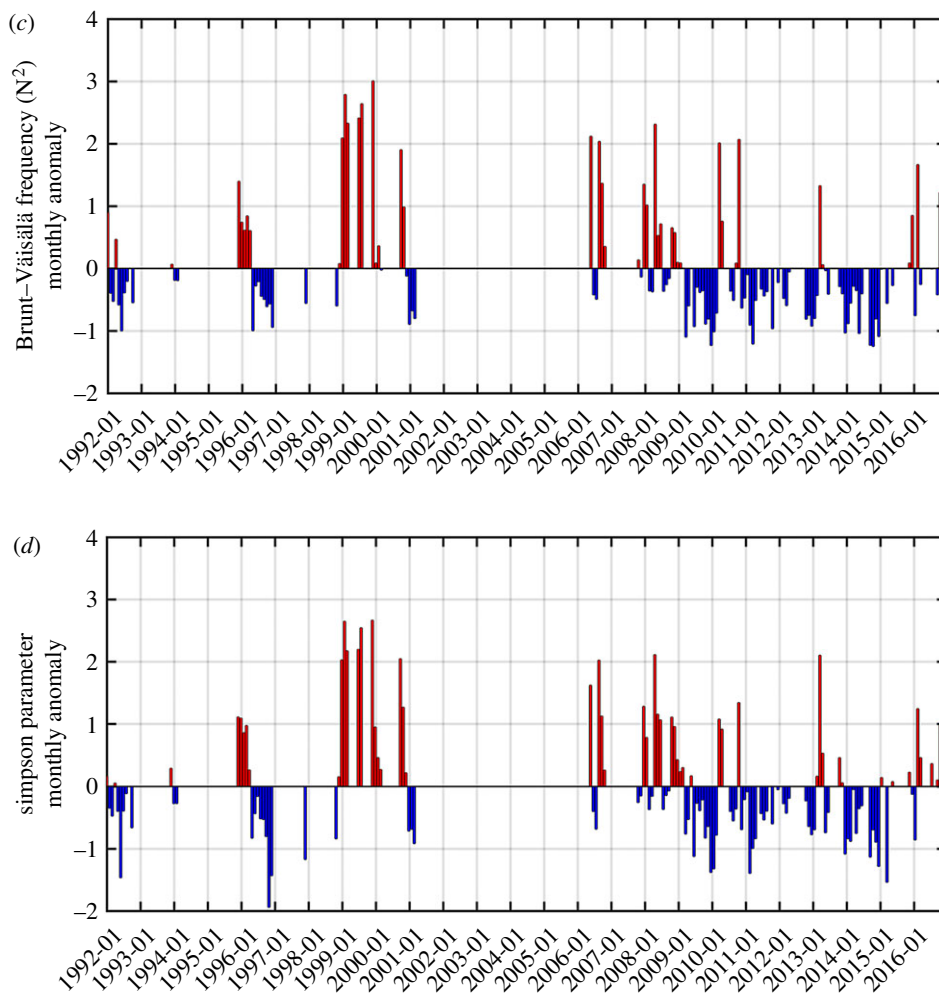


Figure 8. Water-column stability parameters at Rothera Station and Carlini Station (PC). (a) Monthly (standardized) MLD anomalies at Rothera Station and (b) the monthly (standardized) Brunt–Väisälä frequency (N^2) at Carlini Station (PC).

provides a mechanistic basis for the observed decreasing Chl trend there. Our findings on the opposite trends in the phytoplankton biomass along a climate gradient contrast observations by Montes-Hugo *et al.* [32] where phytoplankton biomass significantly decreased in the northern WAP (near Carlini Station (PC)) and increased in the southern WAP (near Rothera Station).

(b) The first case of the empirical orthogonal function analysis: seasonal/inter-annual covariability at individual stations

The first case of the EOF analysis distils the bulk Chl variability into dominant features in seasons (i.e. EOFs) coherent from year to year and represents how the amplitude of each seasonal variability pattern varies over the studied years (i.e. PCs), providing a means to explore the inter-annual variability of seasonal phytoplankton bloom dynamics at each sampling site (e.g. [21]).

All three stations were characterized by distinct phenology of the phytoplankton biomass accumulations, but with greater resemblance in the seasonal progression patterns between Carlini Station (PC) and Rothera Station. The leading modes captured more of the total Chl variability at

Carlini Station (PC) and Rothera Station, whereas relatively the first two modes captured nearly an equal amount of the total Chl variability at Palmer Station (29% by the first mode and 18% by the second mode; figure 5*b*). In addition, at Carlini Station (PC) and Rothera Station, the leading modes represented low-frequency dynamics of Chl, showing fluctuations in the year-round phytoplankton biomass (EOF1, figure 5*a,c*), while seasonally two different phytoplankton blooms (i.e. summer blooms and spring blooms) were observed at Palmer Station (EOF1, figure 5*b*). Phytoplankton species composition has been shown to explain high or low phytoplankton biomass years at Palmer Station, where increased abundance of diatoms was found in high-biomass years and increased abundance of cryptophytes was found in low-biomass years [30]. However, phytoplankton species composition is similar at all three stations [26,31,33,42,44]. As soon as spring ice retreats and water columns are stabilized, diatoms dominate, taking advantage of sufficient irradiance and nutrients, while in the later growing season smaller species like cryptophytes and nanoflagellate species take over the phytoplankton bloom in the glacial melt-induced fresher and warmer water columns [46–53]. In both high and low Chl years at Carlini Station (PC), phytoplankton species composition showed a classical succession pattern with a centric diatom species, *Corethron criophilum*, evolving to a diverse community dominated by *Thalassiosira* and *Porosira* species, and finally turning into a community dominated by the prymnesiophyte *Phaeocystis antarctica* as the main species [42]. In response to glacial melt-induced low-salinity conditions in later growing seasons the abundances of small pennate diatom species (*Navicula glaciei*, *N. perminuta*, *Nitzschia* cf. *lecointei*, *Fragilariopsis cylindrus/nana*) increase, but the species composition does not seem to be significantly affected by the loadings of suspended particulate organic matter [42,54]. Thus, phytoplankton community composition might not explain the observed differences in the EOF/PC patterns of the phytoplankton biomass accumulations at the three sites. Nonetheless, the EOF analysis reveals that the phenology of the phytoplankton blooms was different among the sampling sites.

(c) The second case of the empirical orthogonal function analysis: seasonal/inter-annual-spatial covariability for all three stations together

Compared to the first case of the EOF analysis, the second case of the EOF analysis additionally incorporates the spatial patterns of any two of the three stations into the inter-annual variability of seasonal phytoplankton dynamics at each site. Here, EOF patterns still represent individual sites' inter-annual variability of the seasonal phytoplankton biomass. However, importantly, these EOF patterns are essentially gathered information from site-specific phytoplankton dynamics of which the variability was statistically derived by taking the other two stations' dynamics into account.

Ecologically speaking, the leading mode indicates that, in a seasonally evolving manner, along the latitudinal gradient from Carlini Station (PC) to Rothera Station, if lower (than the 25-year climatology) summer–winter (January–July) and spring (October–November) phytoplankton blooms occur at Carlini Station (PC), it probably co-occurs with or is followed by particularly high winter–early spring (June–September) phytoplankton biomass at Palmer Station. By contrast, this pattern probably co-occurs with the pattern where phytoplankton biomass is consistently low all year-round at Rothera Station (figure 6*a*). This seasonal progression pattern is most evident in the year 2010 shown as the highest PC1 year. Notably, the year 2010 was impacted by the winter La Niña condition. The preceding winter's La Niña condition shapes an environmental configuration for low phytoplankton growth and accumulation in the spring/summer as a consequence of decreased winter sea ice growth, spring sea ice melt and water-column stability [7,29–31]. Indeed, there was an evident relationship between the springtime Chl patterns and water-column stability parameters at Carlini Station (PC) and Rothera Station. At Carlini Station (PC), low phytoplankton biomass in the spring was driven by decreased water-column stability via low N^2 (i.e. negative anomalies in figure 8*b*; $r = 0.60$, $p = 0.063$ for August–September N^2 anomalies versus September–October Chl anomalies). Likewise, low spring phytoplankton biomass at Rothera Station might be caused by decreased water-column stability via deeper MLD (i.e.

positive anomalies in figure 8a; $r = -0.45$, $p = 0.068$ for October MLD anomaly versus October Chl anomaly). The monthly MLD anomalies were persistently positive in the year 2010 at Rothera Station (figure 8a), which might also explain the low year-round phytoplankton biomass in the highest PC1 year. However, high winter–early spring Chl at Palmer Station might be due to diatoms released from within sea ice, given that at Palmer Station La Niña events were associated with early ice retreat and caused significant silicate drawdown in the beginning of the Austral growing season in the absence of increased water-column stability [21]. This is further supported by strong correlations between winter/spring Chl and La Niña conditions at Palmer Station ($r = 0.70$, $p = 0.036$ for August Chl versus August SOI and $r = 0.69$, $p = 0.013$ for September Chl versus August SOI). When La Niña conditions were superimposed on +SAM conditions, Chl increased significantly at Palmer Station (figure 7b). Similar observations were found at Carlini Station (PC) ($r = 0.70$, $p = 0.034$ for August Chl versus August SOI and $r = 0.72$, $p = 0.018$ for September Chl versus August SOI), suggesting that phytoplankton cells might be released from melting sea ice; this might explain positive Chl anomalies in some of the winter months (August) at Carlini Station (PC) (figure 6a). However, such observations were not found at Rothera Station (figure 7b).

Mode 2 contradicts the pattern represented by the leading mode, showing the Chl ‘lows’ (i.e. year-round low Chl) at Carlini Station (PC) and Palmer Station with the Chl ‘high’ (i.e. year-round high Chl) at Rothera Station. This low-frequency dipole pattern of the phytoplankton seasonal progression was not associated with any particular climate modes. However, it is noteworthy that the frequency of this seasonal–spatial phytoplankton variability pattern significantly decreased over the studied years, which implies increases in the year-round Chl at Carlini Station (PC) and Palmer Station and a decrease in the year-round Chl at Rothera Station. Consistent with our findings discussed above (4a Climatology, Monthly Anomalies and Trends), the decreasing PC2 trend was partly influenced by increasing Chl trends at Carlini Station (PC) and Palmer Station, but a decreasing Chl trend at Rothera Station.

5. Conclusion

This study presents the temporally most extensive analysis of phytoplankton biomass in coastal Antarctica, encompassing the results from the three long-term monitoring sites, Carlini Station (PC), Palmer Station and Rothera Station, along the coastal WAP. Importantly, our results shed new light on the relative spatial scales of the different driving mechanisms. Despite their geographical proximity, the three sites were characterized by distinct phenology of phytoplankton biomass accumulation as revealed by EOF analysis (i.e. the first case of the EOF analysis). The spring–summer phytoplankton biomass at Carlini Station (PC) was notably lower compared with Palmer Station and Rothera Station, presumably due to the local effect of particles derived from glacier melt shading phytoplankton cells at Potter Cove during the growth season, especially in warmer years. There were significant trends towards increased monthly Chl anomalies for the studied years at Carlini Station (PC) and Palmer Station. By contrast, phytoplankton biomass decreased significantly for the studied years at Rothera Station, which appears to be related to the increasing MLD trend at Rothera Station. The three sampling stations are situated close to each other when considering the spatial scale of large-scale climate forcing; however, there were inconsistent responses of the magnitudes of winter and spring phytoplankton biomass to distinct ENSO and SAM regimes among the three stations. This observation suggests a significant role of local-scale forcings (e.g. retreating glaciers and topographically steered circulation) which additionally contribute to shaping phytoplankton blooms along the three stations. The inter-annual variability of the seasonal phytoplankton biomass derived from all three stations together (i.e. the second case of the EOF analysis) presented ecologically meaningful patterns, which were explained by an opposing set of climate and physical forcing mechanisms. Mode 1 captured seasonally co-occurring patterns of low summer–winter and spring Chl at Carlini Station (PC), high winter–early spring Chl at Palmer Station and low year-round Chl at Rothera Station. Mode 1 also demonstrated that the most dominant seasonal Chl patterns were directly influenced by the

magnitude of water-column stability, which in turn was governed by ENSO and the SAM. Mode 2 captured the year-round low Chl at Carlini Station (PC) and Palmer Station but high Chl at Rothera Station, of which the frequency decreased significantly in conjunction with increasing Chl trends at Carlini Station (PC) and Palmer Station and the decreasing Chl trend at Rothera Station.

In recent decades, the WAP has responded dramatically to climate change at rates faster than any other ecosystems in the Southern Hemisphere, which has resulted in significant responses of marine ecological functions and food-web processes. As observed in our study, long-term trends in phytoplankton biomass were evident along the coastal WAP. The long-term changes in phytoplankton, in turn, impact upper trophic levels (e.g. Antarctic krill and penguin populations) as well as microbial loop components (e.g. heterotrophic bacteria), leading to changes in carbon flow among the WAP food-web components and, ultimately, carbon export.

Data accessibility. Primary data used in the present study can be assessed as follows. Carlini Station (PC): PANGAEA depository (<https://issues.pangaea.de/browse/PDI-14850>), Palmer Station: Palmer LTER Datazoo (<http://pal.lternet.edu/data>; Dataset 177; (doi:10.6073/pasta/f597726f6bb68980ea3c0e7461f298b3)) and Rothera Station: British Oceanographic Data Centre (<http://www.bodc.ac.uk/data>).

Authors' contributions. H.K. performed data analysis and drafted the manuscript. H.W.D., P.D.R. and I.R.S. helped the design of the study and analysis. H.W.D., D.A., E.R.B., A.G.J.B., M.P.M., P.D.R., O.M.S., H.J.V. and I.R.S. acquired data, carried out experiments and measurements, and helped with interpretation of data. All the authors read and approved the manuscript.

Competing interests. We declare we have no competing interests.

Funding. Palmer Long Term Ecological Research (LTER) Project was supported by US National Science Foundation awards OPP-9011927, 9632763, 0217282, 0823101 and GEO-PLR 1440435. H.K. was supported as a Postdoctoral Research Scientist by Lamont-Doherty Earth Observatory (LDEO) of Columbia University and by a subcontract to LDEO from NASA ROSES award NNX14AL86G to S. Doney (Woods Hole Oceanographic Institution/University of Virginia). Rothera Time Series (RaTS) is a component of the British Antarctic Survey (BAS) Polar Oceans programme, funded by the Natural Environment Research Council. Carlini ecological long-term research is conducted in the frame of the collaboration between the Argentine Antarctic Institute (IAA) and the Alfred Wegener Institute (Germany). This work was supported by the EU research network IMCONet funded by the Marie Curie Action IRSES (FP7 IRSES, Action No. 318718).

Acknowledgements. We thank the many current and former team members for their assistance with field sampling, processing and analysing the chlorophyll samples from Carlini Station (PC), Palmer Station and Rothera Station. Laura Gerrish (BAS) is thanked for help with figure preparation.

References

1. King JC. 1994 Recent climate variability in the vicinity of the Antarctic Peninsula. *Int. J. Climatol.* **14**, 357–369. (doi:10.1002/joc.3370140402)
2. Smith RC, Stammerjohn SE, Baker KS. 1996 *Surface air temperature variations in the Western Antarctic Peninsula region, in Foundations for Ecological Research West of the Antarctic Peninsula*, pp. 105–121. Washington, DC: AGU.
3. Meredith MP, King JC. 2005 Rapid climate change in the ocean to the west of the Antarctic Peninsula during the second half of the 20th century. *Geophys. Res. Lett.* **32**, L19604. (doi:10.1029/2005GL024042)
4. Whitehouse MJ, Meredith MP, Rothery P, Atkinson A, Ward P, Korb RE. 2008 Rapid warming of the ocean around South Georgia, Southern Ocean during the 20th Century: forcings, characteristics and implications for lower trophic levels. *Deep Sea Res. I, Top. Stud. Oceanogr.* **55**, 1218–1228. (doi:10.1016/j.dsr.2008.06.002)
5. Clarke A, Griffiths HJ, Barnes DKA, Meredith MP, Grant SM. 2009 Spatial variation in seabed temperatures in the Southern Ocean: implications for benthic ecology and biogeography. *J. Geophys. Res.* **114**, G03003.
6. Vaughan DG, Marshall GJ, Connolley WM, Parkinson C, Mulvaney R, Hodgson DA, King JC, Pudsey CJ, Turner J. 2003 Recent rapid regional climate warming on the Antarctic Peninsula. *Clim. Change* **60**, 243–274. (doi:10.1023/A:1026021217991)
7. Stammerjohn SE, Martinson DG, Smith RC, Yuan X, Rind D. 2008 Trends in Antarctic annual sea ice retreat and advance and their relation to El Niño-Southern Oscillation and

- Southern Annular Mode variability. *J. Geophys. Res.* **113**, 4603. (doi:10.1029/2007JC004269)
8. Cook AJ, Fox AJ, Vaughan DG, Ferrigno JG. 2005 Retreating glacier fronts on the Antarctic Peninsula over the past half-century. *Science* **308**, 541–544. (doi:10.1126/science.1104235)
 9. Vaughan DG. 2006 Recent trends in melting conditions on the Antarctic Peninsula and their implications for ice-sheet mass balance and sea level. *Arct. Antarct. Alp. Res.* **38**, 147–152. (doi:10.1657/1523-0430(2006)038[0147:RTIMCO]2.0.CO;2)
 10. Weston K, Jickells TD, Carson DS, Clarke A, Meredith MP, Brandon MA, Wallace MI, Ussher SJ, Hendry KR. 2013 Primary production export flux in Marguerite Bay (Antarctic Peninsula): linking upper water-column production to sediment trap flux. *Deep Sea Res. I, Top. Stud. Oceanogr.* **75**, 52–66. (doi:10.1016/j.dsr.2013.02.001)
 11. Martinson DG, Stammerjohn SE, Iannuzzi RA, Smith RC, Vernet M. 2008 Western Antarctic Peninsula physical oceanography and spatio-temporal variability. *Deep Sea Res. II, Top. Stud. Oceanogr.* **55**, 1964–1987. (doi:10.1016/j.dsr2.2008.04.038)
 12. Massom RA *et al.* 2006 Extreme anomalous atmospheric circulation in the West Antarctic Peninsula region in austral spring and summer 2001/02, and its profound impact on sea ice and biota. *J. Clim.* **19**, 3544–3571. (doi:10.1175/JCLI3805.1)
 13. Gong DY, Wang SW. 1999 Definition of antarctic oscillation index. *Geophys. Res. Lett.* **26**, 459–462. (doi:10.1029/1999GL900003)
 14. Marshall GJ, Orr A, van Lipzig N, King J. 2006 The impact of a changing Southern Hemisphere annular mode on Antarctic Peninsula summer temperatures. *J. Clim.* **19**, 5388–5404. (doi:10.1175/JCLI3844.1)
 15. Ducklow HW, Baker K, Martinson DG, Quetin LB, Ross RM, Smith RC, Stammerjohn SE, Vernet M, Fraser W. 2007 Marine pelagic ecosystems: the West Antarctic Peninsula. *Phil. Trans. R. Soc. B* **362**, 67–94. (doi:10.1098/rstb.2006.1955)
 16. Edwards R, Sedwick P. 2001 Iron in East Antarctic snow: implications for atmospheric iron deposition and algal production in Antarctic waters. *Geophys. Res. Lett.* **28**, 3907–3910. (doi:10.1029/2001GL012867)
 17. Raiswell R. 2011 Iceberg-hosted nanoparticulate Fe in the Southern Ocean mineralogy, origin, dissolution kinetics and source of bioavailable Fe. *Deep Sea Res. II, Top. Stud. Oceanogr.* **58**, 1364–1375. (doi:10.1016/j.dsr2.2010.11.011)
 18. Serebrennikova YM, Fanning KA. 2004 Nutrients in the Southern Ocean GLOBEC region: variations. *Water circulation, and cycling. Deep Sea Res. II, Top. Stud. Oceanogr.* **51**, 1981–2002. (doi:10.1016/j.dsr2.2004.07.023)
 19. Ducklow H *et al.* 2012 The marine system of the Western Antarctic Peninsula. In *Antarctic ecosystems: an extreme environment in a changing world* (ed. AD Rogers, NM Johnston, EJ Murphy, A Clarke), pp. 121–159. Oxford, UK: Blackwell Publishing.
 20. Annett AL, Henley SF, Van Beek P, Souhaut M, Ganeshram R, Venables HJ, Meredith MP, Geibert W. 2013 Use of radium isotopes to estimate mixing rates and trace sediment inputs to surface waters in northern Marguerite Bay, Antarctic Peninsula. *Antarct. Sci.* **25**, 445–456. (doi:10.1017/S0954102012000892)
 21. Kim H, Doney SC, Iannuzzi RA, Meredith MP, Martinson DG, Ducklow HW. 2016 Climate forcing for dynamics of dissolved inorganic nutrients at Palmer Station, Antarctica: an interdecadal (1993–2013) analysis. *J. Geophys. Res. Biogeosci.* **121**, 2369–2389. (doi:10.1002/2015JG003311)
 22. Carvalho F, Kohut J, Oliver MJ, Sherrell RM, Schofield O. 2016 Mixing and phytoplankton dynamics in a submarine canyon in the West Antarctic Peninsula. *J. Geophys. Res.* **121**, 5069–5083.
 23. Smith RC, Baker KS, Vernet M. 1998 Seasonal and interannual variability of phytoplankton biomass west of the Antarctic Peninsula. *J. Mar. Syst.* **17**, 229–243. (doi:10.1016/S0924-7963(98)00040-2)
 24. Clarke A, Meredith MP, Wallace MI, Brandon MA, Thomas DN. 2008 Seasonal and interannual variability in temperature, chlorophyll and macronutrients in Ryder Bay, northern Marguerite Bay, Antarctica. *Deep Sea Res. II, Top. Stud. Oceanogr.* **55**, 1988–2006. (doi:10.1016/j.dsr2.2008.04.035)
 25. Vernet MD, Martinson G, Iannuzzi RA, Stammerjohn S, Kozlowski W, Sines K, Smith R, Garibotti I. 2008 Primary production within the sea-ice zone west of the Antarctic Peninsula:

- I—Sea ice, summer mixed layer, and irradiance. *Deep Sea Res. II, Top. Stud. Oceanogr.* **55**, 2068–2085. (doi:10.1016/j.dsr2.2008.05.021)
26. Schloss IR, Abele D, Moreau S, Demers S, Bers AV, Gonzalez O, Ferreyra GA. 2012 Response of phytoplankton dynamics to 19-year (1991–2009) climate trends in Carlini Station (Antarctica). *J. Mar. Syst.* **92**, 53–66. (doi:10.1016/j.jmarsys.2011.10.006)
 27. Ducklow HW *et al.* 2013 West Antarctic Peninsula: an ice-dependent coastal marine ecosystem in transition. *Oceanography* **26**, 190–203. (doi:10.5670/oceanog.2013.62)
 28. Schloss IR *et al.* 2014 On the phytoplankton bloom in coastal waters of southern King George Island (Antarctica) in January 2010: an exceptional feature? *Limnol. Oceanogr.* **59**, 195–210. (doi:10.4319/lo.2014.59.1.0195)
 29. Venables HJ, Clarke A, Meredith MP. 2013 Wintertime controls on summer stratification and productivity at the Western Antarctic Peninsula. *Limnol. Oceanogr.* **58**, 3:1035–1047.
 30. Saba GK *et al.* 2014 Winter and spring controls on the summer food web of the coastal West Antarctic Peninsula. *Nat. Commun.* **5**, 4318.
 31. Rozema PD, Venables HJ, Poll WH, Clarke A, Meredith MP, Buma AGJ. 2016 Interannual variability in phytoplankton biomass and species composition in northern Marguerite Bay (West Antarctic Peninsula) is governed by both winter sea ice cover and summer stratification. *Limnol. Oceanogr.* **62**, 235–252. (doi:10.1002/lno.10391)
 32. Montes-Hugo M, Doney SC, Ducklow HW, Fraser W, Martinson D, Stammerjohn SE, Schofield O. 2009 Recent changes in phytoplankton communities associated with rapid regional climate change along the western Antarctic Peninsula. *Science* **323**, 1470–1473. (doi:10.1126/science.1164533)
 33. Schofield O *et al.* 2017 Decadal variability in coastal phytoplankton community composition in a changing West Antarctic Peninsula. *Deep Sea Res. I, Top. Stud. Oceanogr.* **124**, 42–54. (doi:10.1016/j.dsr.2017.04.014)
 34. Wöflf AC, Lim CH, Hass HC, Lindhorst S, Tosonotto G, Lettmann K, Kuhn G, Wolff J-O, Abele D. 2014 Classification of marine periglacial habitats based on hydroacoustic data and bed shear stress estimations (Potter Cove, King George Island, Antarctica). *Mar. Geol. Lett.* **34**, 435–446. (doi:10.1007/s00367-014-0375-1)
 35. Monien D, Monien P, Brünjes R, Widmer T, Kappenberg A, Busso AAS, Schnetger B, Brumsack HJ. 2017 Meltwater as a source of potentially bioavailable iron to Antarctica waters. *Antarct. Sci.* **29**, 272–291.
 36. Wöflf A-C, Wittenberg N, Feldens P, Hass HC, Betzler C, Kuhn G. 2016 Submarine landforms related to glacier retreat in a shallow Antarctic fjord. *Antarct. Sci.* **28**, 475–486.
 37. Schloss IR, Ferreyra GA. 2002 Primary production, light and vertical mixing in Carlini Station, a shallow coastal Antarctic environment. *Polar Biol.* **25**, 41–48. (doi:10.1007/s003000100309)
 38. Pakulski JD, Kase JP, Meador JA, Jeffrey WH. 2008 Effect of stratospheric ozone depletion and enhanced ultraviolet radiation on marine bacteria at Palmer Station, Antarctica in the early austral spring. *Photochem. Photobiol.* **84**, 215–221.
 39. Annett AL, Skiba M, Henley SF, Venables HJ, Meredith MP, Statham PJ, Ganeshram RS. 2015 Comparative roles of upwelling and glacial iron sources to Ryder Bay, coastal western Antarctic Peninsula. *Mar. Chem.* **176**, 21–33. (doi:10.1016/j.marchem.2015.06.017)
 40. Annett AL, Fitzsimmons JN, Seguret MJM, Lagerstrom M, Meredith MP, Schofield O, Sherrell RM. 2017 Control on dissolved and particulate iron distributions in surface waters of the Western Antarctic Peninsula shelf. *Mar. Chem.* **196**, 81–97. (doi:10.1016/j.marchem.2017.06.004)
 41. Varela L. 1998 Hydrology of Matías and Potter Creeks. In *The carlini station coastal ecosystem, Antarctica*. *Ber. Polarforsch.*, vol. 299 (eds C Wiencke, GA Ferreyra, W Arntz, C Rinaldi), pp. 33–39. Karl Kamloth: Bremen.
 42. Schloss IR, Ferreyra GA, Ruiz-Pino D. 2002 Phytoplankton Biomass in Antarctic Shelf Zones: a conceptual model based on Carlini Station, King George Island. *J. Mar. Sys.* **36**, 129–143. (doi:10.1016/S0924-7963(02)00183-5)
 43. Poigner H, Wilhelms-Dick D, Abele D, Staubwasser M, Henkel S. 2015 Iron assimilation by the clam *Laternula elliptica*: do stable isotopes ($\delta^{56}\text{Fe}$) help to decipher the sources? *Chemosphere* **134**, 294–300. (doi:10.1016/j.chemosphere.2015.04.067)
 44. Van de Poll WH, Lagunas M, de Vries T, Visser RJ, Buma AJ. 2011 Non-photochemical quenching of chlorophyll fluorescence and xanthophyll cycle responses after excess PAR and

- UVR in *Chaetoceros brevis*, *Phaeocystis antarctica* and coastal Antarctic phytoplankton. *Mar. Ecol. Prog. Ser.* **426**, 119–131. (doi:10.3354/meps09000)
45. Bers AV, Momo F, Schloss I, Abele D. 2013 Analysis of trends and sudden changes in environmental long-term data from King George Island (Antarctica): relationships between global climatic oscillations and local system response. *Clim. Change* **116**, 789–803. (doi:10.1007/s10584-012-0523-4)
 46. Villafañe V, Helbling EW, Holm-Hansen O. 1993 Phytoplankton around Elephant Island, Antarctica. *Polar Biol.* **13**, 183–191. (doi:10.1007/BF00238928)
 47. Moline MA, Prezelin BB. 1996 Palmer LTER 1991–1994: Long-term monitoring and analyses of physical factors regulating variability in coastal Antarctic phytoplankton biomass, in situ productivity and taxonomic composition over subseasonal, seasonal and interannual time scales phytoplankton dynamics. *Mar. Ecol. Prog. Ser.* **145**, 143–160. (doi:10.3354/meps145143)
 48. Moline MA, Claustre H, Frazer TK, Grzymyskj J, Schofield O, Vernet M. 2001 Changes in phytoplankton assemblages along the Antarctic Peninsula and potential implications for the Antarctic food web.
 49. Dierssen HM, Smith RC, Vernet M. 2002 Glacial meltwater dynamics in coastal waters west of the Antarctic Peninsula. *Proc. Natl Acad. Sci. USA* **99**, 1790–1795. (doi:10.1073/pnas.032206999)
 50. Moline MA, Claustre H, Frazer TK, Schofield O, Vernet M. 2004 Alteration of the food web along the Antarctic Peninsula in response to a regional warming trend. *Glo. Change Biol.* **10**, 1973–1980. (doi:10.1111/j.1365-2486.2004.00825.x)
 51. Garibotti IA, Vernet M, Kozlowski WA, Ferrario ME. 2003 Composition and biomass of phytoplankton assemblages in coastal Antarctic waters: a comparison of chemotaxonomic and microscopic analyses. *Mar. Ecol. Prog. Ser.* **247**, 27–42. (doi:10.3354/meps247027)
 52. Garibotti IA, Vernet M, Smith RC, Ferrario ME. 2005 Interannual variability in the distribution of the phytoplankton standing stock across the seasonal sea-ice zone west of the Antarctic Peninsula. *J. Plankton Res.* **27**, 825–843. (doi:10.1093/plankt/fbi056)
 53. Kozlowski WA. 2008 Pigment derived phytoplankton composition along the Western Antarctic Peninsula. MS thesis, San Diego State University, San Diego, CA, USA.
 54. Hernando MP, Schloss IR, Malanga GF, Almandoz GO, Ferreyra GA, Aguiar MB, Puntarulo S. 2015 Effects of salinity changes on coastal Antarctic phytoplankton physiology and assemblage composition. *J. Exp. Mar. Biol. Ecol.* **466**, 110–119. (doi:10.1016/j.jembe.2015.02.012)